

## Electronic Supplementary Information (ESI) for

### **An endoplasmic reticulum-targeting iridium(III) complex induces immunogenic cell death in melanoma cells and enhances anti-PD-1 immunotherapy by remodeling tumor microenvironment**

Yi Rong<sup>a</sup>, Zhongxian Fan<sup>b</sup>, Zhijie Yu<sup>a</sup>, Li Wei<sup>b</sup>, Han Shen<sup>a</sup>, Huaiyi Huang<sup>b</sup>, Xiaojuan Hao<sup>ac</sup>, Zizhuo Zhao<sup>d</sup>, Jinqun Wang<sup>a\*</sup>

<sup>a</sup>Guangdong Provincial Key Laboratory of Advanced Drug Delivery, School of Bioscience and Biopharmaceutics, Guangdong Pharmaceutical University, Guangzhou, 510006, P. R. China. E-mail: wangjinqun@gdpu.edu.cn

<sup>b</sup>School of Pharmaceutical Science (Shenzhen), Shen Zhen Campus of Sun Yat-sen University, Shenzhen, 518107, P. R. China.

<sup>c</sup>Wenzhou Institute, University of Chinese Academy of Sciences, Wenzhou, Zhejiang 325001, P. R. China.

<sup>d</sup>Department of Ultrasound, Sun Yat-Sen Memorial Hospital, Sun Yat-Sen University, Guangzhou, 510275, P. R. China.

#### **List of contents**

#### **Synthesis and characterization of IrC**

**Fig. S1** ESI-MS spectrum of IrC

**Fig. S2** <sup>1</sup>H NMR spectrum of IrC

**Fig. S3** The stability analysis of IrC in the fetal bovine serum (FBS).

**Fig. S4** Cytotoxicity and hallmarks of ICD in A375 cells treated with IrC or oxaliplatin.

**Fig. S5** Cytotoxicity and hallmarks of ICD in B16-F10 cells treated with IrC or oxaliplatin.

**Fig. S6** IrC induces cytotoxicity, cell apoptosis, and ROS, and its cellular localization in B16-F10 melanoma cells.

**Fig. S7** Hallmarks of ER stress and ICD in B16-F10 cells treated with IrC or CDDP.

**Fig. S8** Body weight curves of the mice in the vaccine experiment.

**Fig. S9** H&E staining of the main organ slices collected from the mice of each group in the vaccine experiment.

**Fig. S10** Proportions of T<sub>EM</sub> cells and T<sub>CM</sub> cells in the PBMC or spleens.

**Fig. S11** H&E staining of the main organ slices collected from the mice under different treatment.

**Fig. S12** Hemolysis assay of IrC with different concentrations.

**Synthesis and characterization of IrC:** IrC was prepared by treating  $[\text{Ir}(\text{ppy})_2\text{Cl}]_2$  with 2 equivalents of  $\text{tpy-ph}(\text{CF}_3)_2$  ligand in  $\text{CHCl}_3/\text{MeOH}$  (2:1; v/v) under refluxing condition (at 60 °C) for 18 h. The solvent of the reaction mixture was removed by distillation under reduced pressure, and the resulting solids were extracted with dichloromethane and water. The organic layer was collected and removed under vacuum. The obtained crude product was further purified by column chromatography on neutral alumina (solvent: methanol/dichloromethane = 1/20). Yield: 70%.  $^1\text{H}$  NMR (400 MHz, Chloroform-*d*)  $\delta$  10.06 (d, 1H), 9.94 (s, 1H), 8.82 (d, 1H), 8.68 (s, 2H), 8.40 (t, 1H), 8.26 (d, 1H), 8.01 (s, 1H), 7.91 – 7.76 (m, 4H), 7.71 (d, 1H), 7.58 (m, 2H), 7.54 (d, 1H), 7.40 – 7.31 (m, 2H), 7.16 (t, 1H), 7.09 (m, 2H), 7.00 – 6.86 (m, 2H), 6.77 (t, 1H), 6.63 (t, 1H), 6.54 (d, 1H), 6.35 (t, 1H), 5.88 (d,  $J = 7.7$  Hz, 1H), 5.50 (d,  $J = 7.6$  Hz, 1H).  $\text{C}_{45}\text{H}_{28}\text{IrN}_5\text{F}_6^+$ : 946.20, found: 946.28. Anal. calc. for  $\text{C}_{45}\text{H}_{29}\text{ClIrN}_5$ : C, 55.07; H, 2.98; N, 7.14. Found: C, 54.90; H, 2.79; N, 7.06.

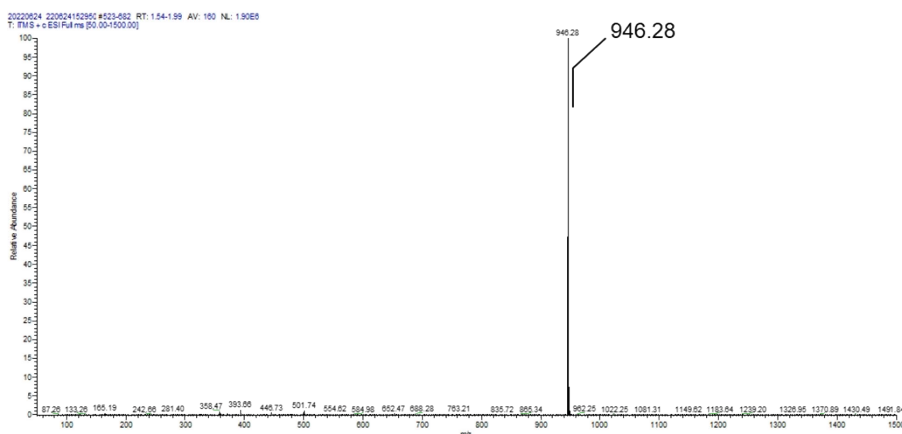


**Fig. S1** ESI-MS spectrum of IrC

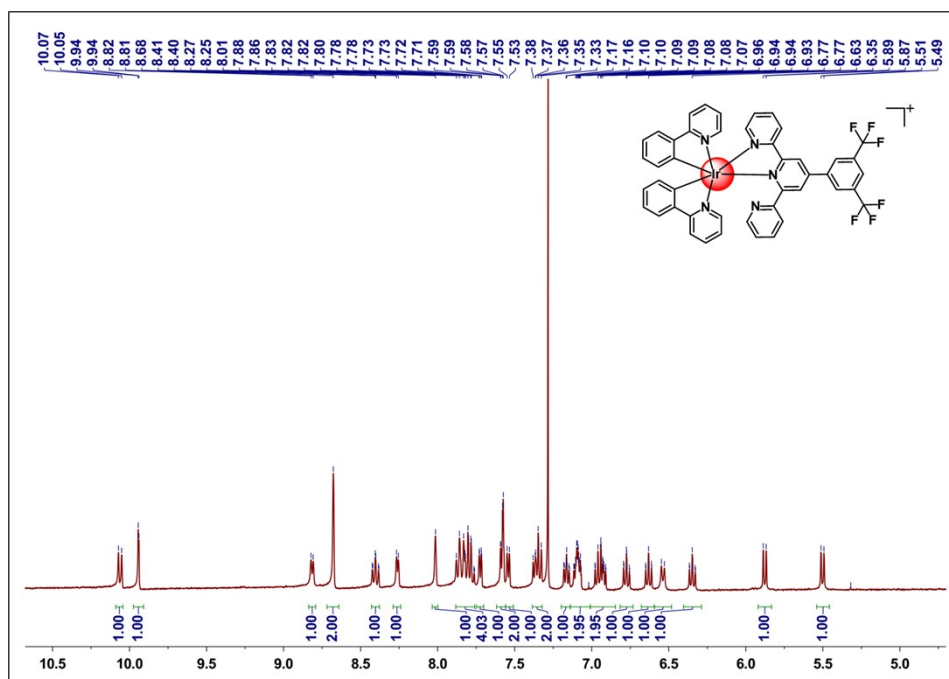


**Fig. S2**  $^1\text{H}$  NMR spectrum of IrC

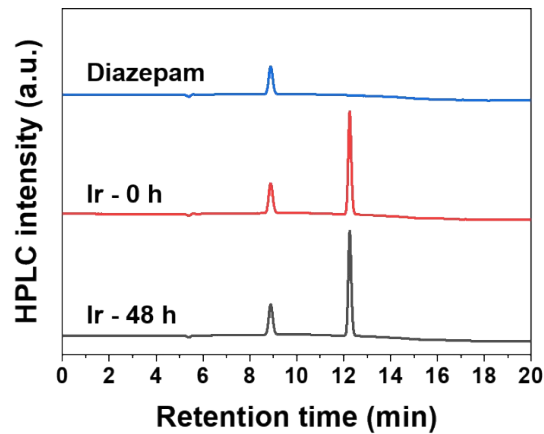


**Fig. S3** The stability analysis of IrC in the fetal bovine serum (FBS).

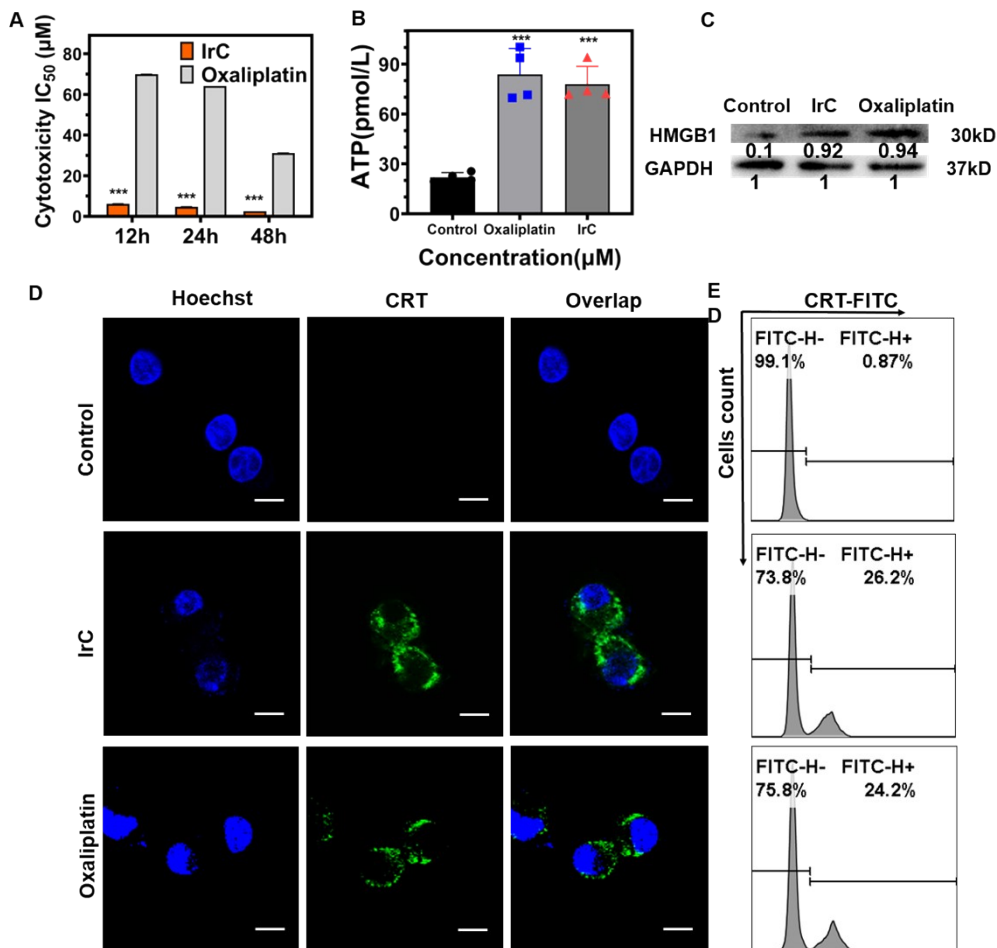


**Fig. S4** Cytotoxicity and hallmarks of ICD in A375 cells treated with IrC (6 µM) or oxaliplatin (70 µM). (A) Half inhibitory concentrations (IC<sub>50</sub>) of IrC and oxaliplatin in A375 cells (B) The extracellular release of ATP after IrC and oxaliplatin treatment. (C) The extracellular HMGB1 in the medium supernatant was detected by Western blot. (D) CLSM images of CRT on cell surface. Scale bars: 50 µm. (E) The quantitative

evaluation of CRT exposure was detected by flow cytometry. \*\*\* =  $P < 0.001$ , compared with the control group.

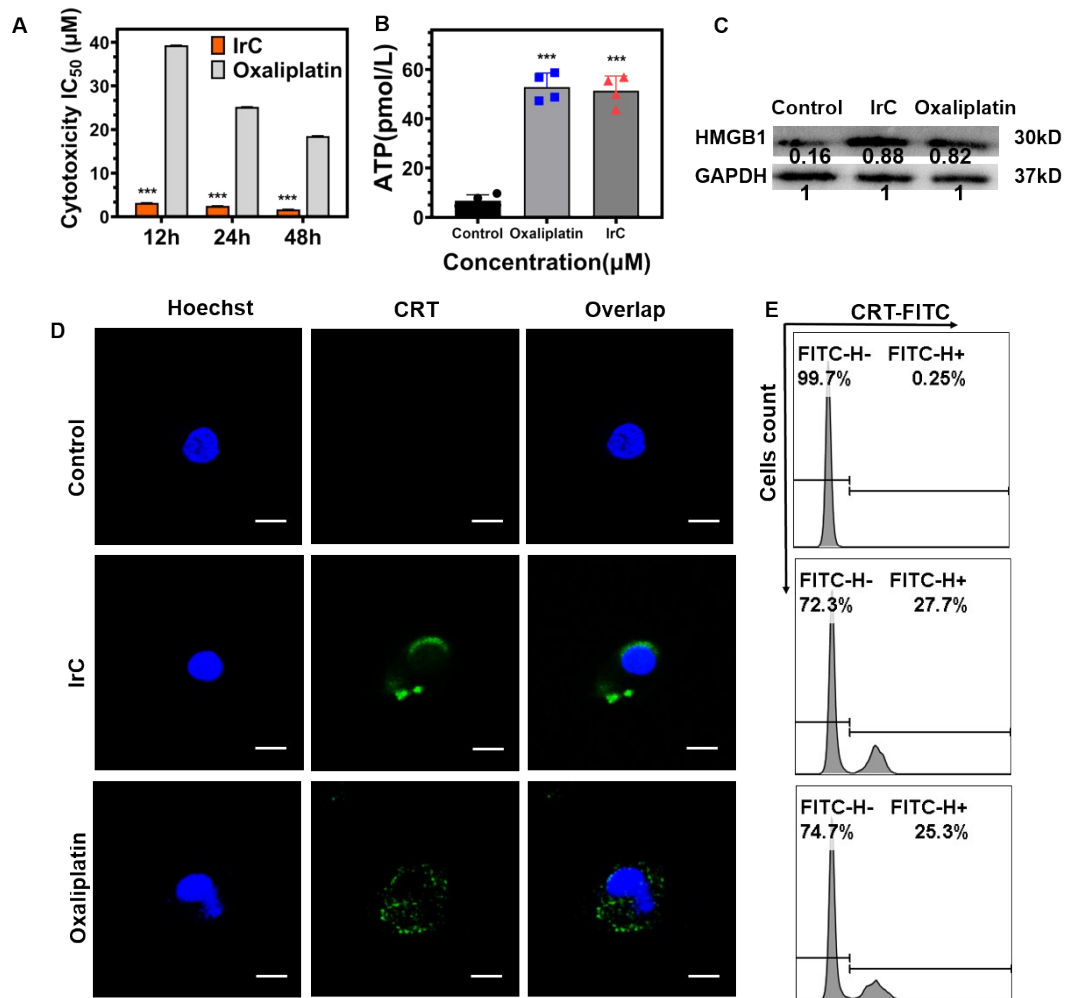


**Fig. S5** Cytotoxicity and hallmarks of ICD in B16-F10 cells treated with IrC (3  $\mu\text{M}$ ) or oxaliplatin (40  $\mu\text{M}$ ). (A) Half inhibitory concentrations ( $IC_{50}$ ) of IrC and oxaliplatin in B16-F10 cells (B) The extracellular release of ATP after IrC and oxaliplatin treatment. (C) The extracellular HMGB1 in the medium supernatant was detected by Western blot. (D) CLSM images of CRT on cell surface. Scale bars: 50  $\mu\text{m}$ . (E) The quantitative evaluation of CRT exposure was detected by flow cytometry. \*\*\* =  $P < 0.001$ , compared with the control group.

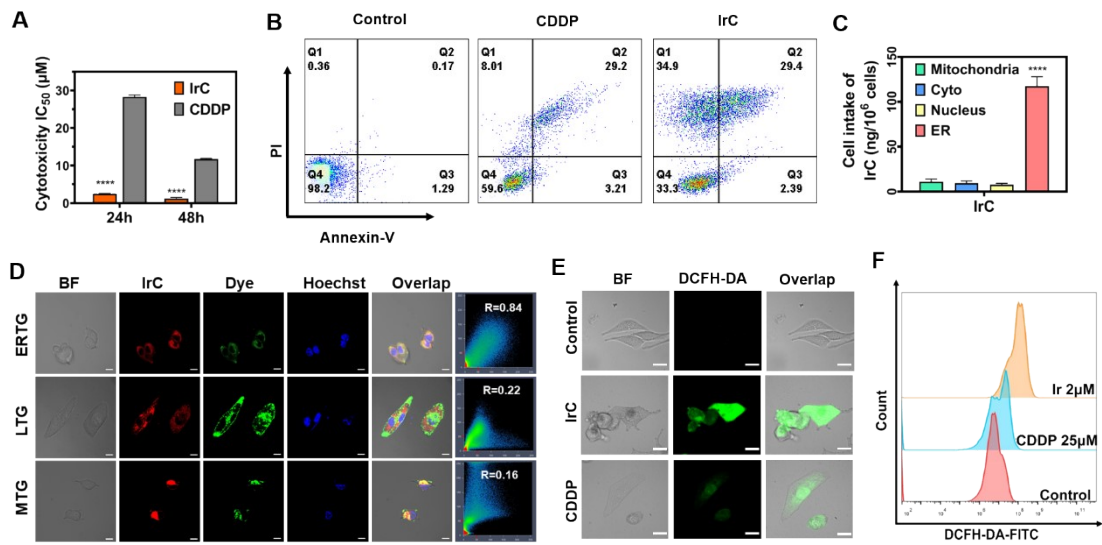


**Fig. S6** IrC induces cytotoxicity, cell apoptosis, and ROS, and its cellular localization in B16-F10 melanoma cells. (A) Half inhibitory concentrations ( $IC_{50}$ ) of IrC and CDDP in B16-F10 cells. (B) Apoptosis determined by flow cytometry with annexin V/PI co-staining assay. (C) Cellular uptake of IrC in the nucleus, lysosomes, mitochondria and ER of B16-F10 cells was quantified by ICP-MS. (D) Co-localization of IrC in B16-F10 cells by CLSM. MTG: Mito-tracker™ Green, ERTG: ER-Tracker™ Green, LTG: Lyso-Tracker™ Green. (E) IrC and CDDP induces ROS generation in the B16-F10 cells detected by CLSM. (F) Detection of ROS by Flow cytometry. Scale bar: 50  $\mu$ m.

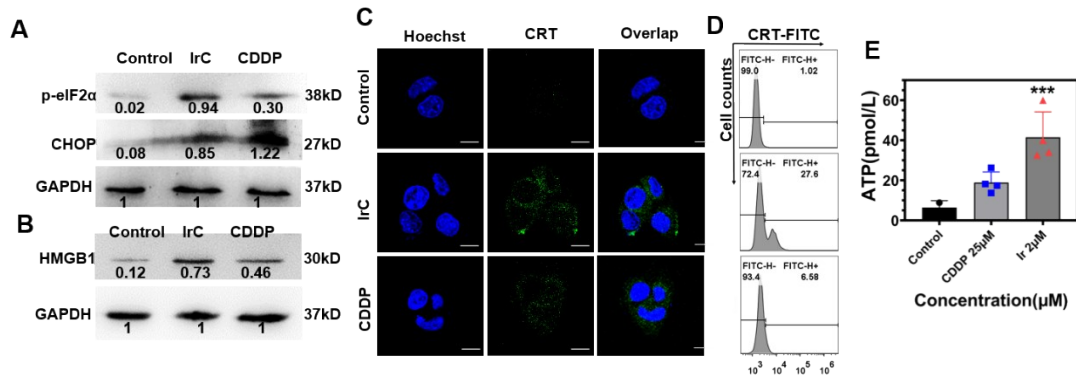


**Fig. S7** Hallmarks of ER stress and ICD in B16-F10 cells treated with IrC (2  $\mu$ M) or CDDP (25  $\mu$ M). (A) The expression of p-eIF2 $\alpha$  and CHOP. (B) The extracellular HMGB1 in the medium supernatant was detected by Western blot. (C) CLSM images of CRT on cell surface. Scale bars: 50  $\mu$ m. (D) The quantitative evaluation of CRT exposure in B16-F10 cells treated with IrC (2  $\mu$ M) or CDDP (25  $\mu$ M) for 12 h was detected by flow cytometry. (E) The release of ATP into the extracellular milieu after IrC and CDDP treatment. \*\*\* =  $P < 0.001$ , compared with the control group.

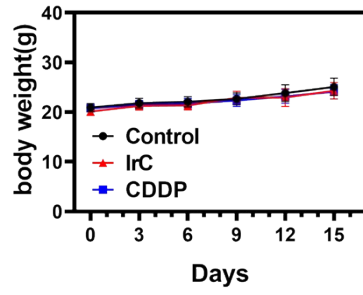


**Fig. S8** Body weight curves of the mice in the vaccine experiment.

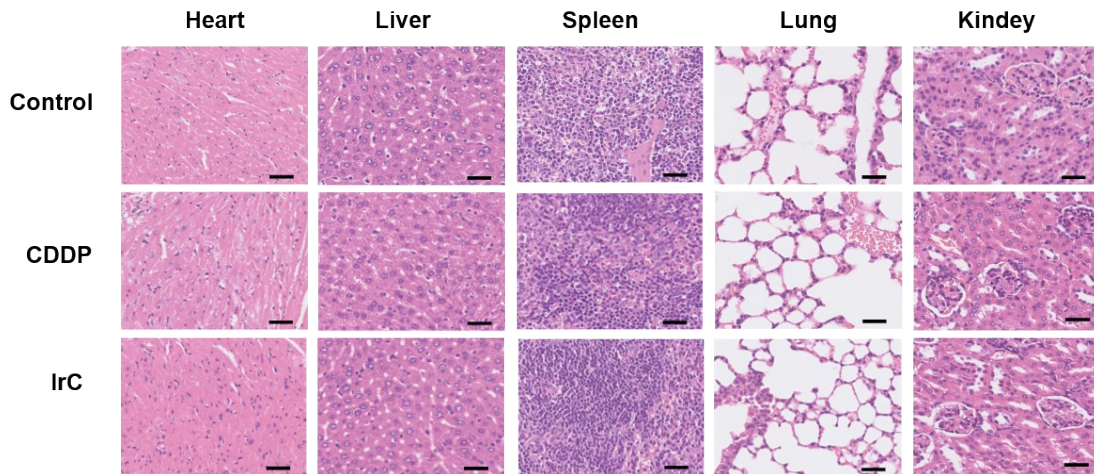


**Fig. S9** H&E staining of the main organ slices collected from the mice of each group in the vaccine experiment. Scale bar is 100 µm.

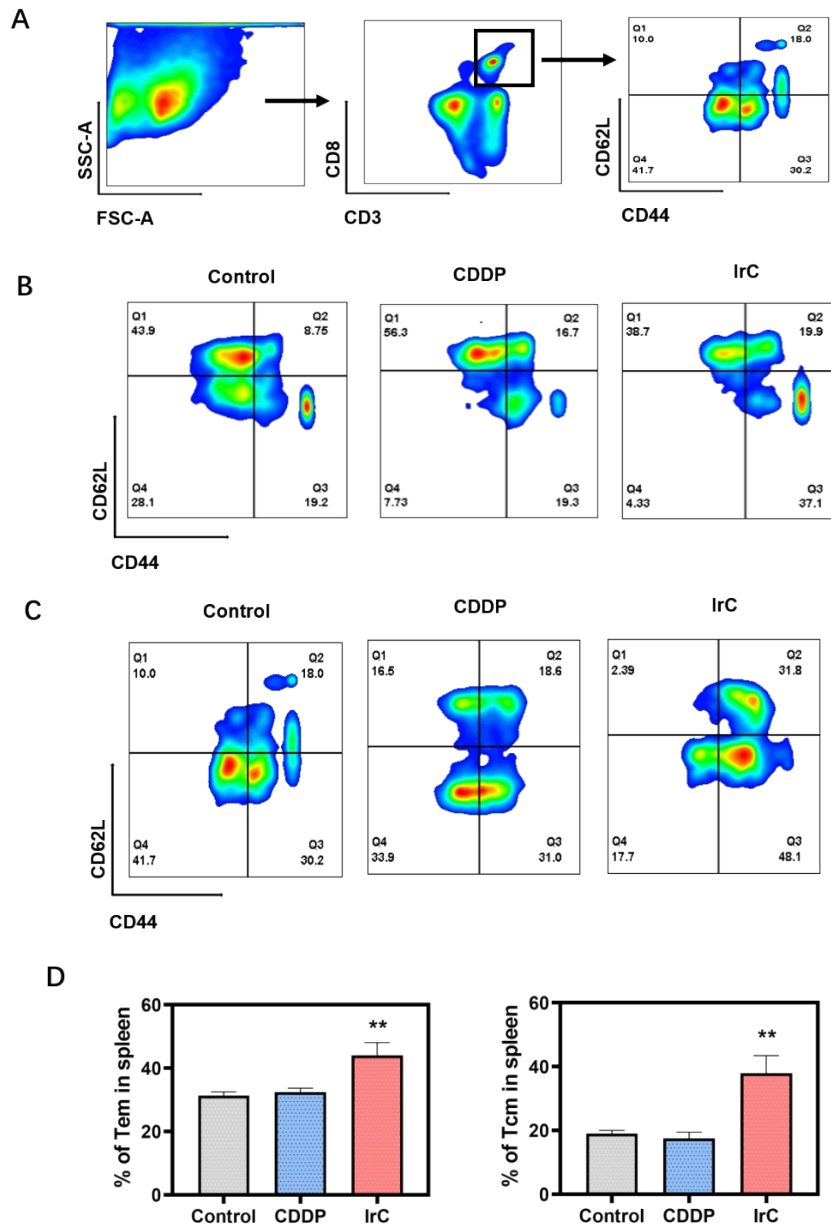


**Fig. S10** Proportions of T<sub>EM</sub> cells and T<sub>CM</sub> cells in the PBMC or spleens. (A) Gating strategies used for cell sorting, representative flow cytometric plots of T<sub>CM</sub> (CD3<sup>+</sup>CD8<sup>+</sup>CD44<sup>+</sup>CD62L<sup>+</sup>) and T<sub>EM</sub> (CD3<sup>+</sup>CD8<sup>+</sup>CD44<sup>+</sup>CD62L<sup>-</sup>). (B) Proportions of T<sub>EM</sub> cells and T<sub>CM</sub> cells in the PBMC (C) Proportions of T<sub>EM</sub> cells and T<sub>CM</sub> cells in the spleens. (D) The quantification of T<sub>EM</sub> and T<sub>CM</sub> cells in the spleens. Data represent mean  $\pm$  SD (n = 3 biologically independent samples), \*\* =  $P < 0.01$ , compared with the control group.

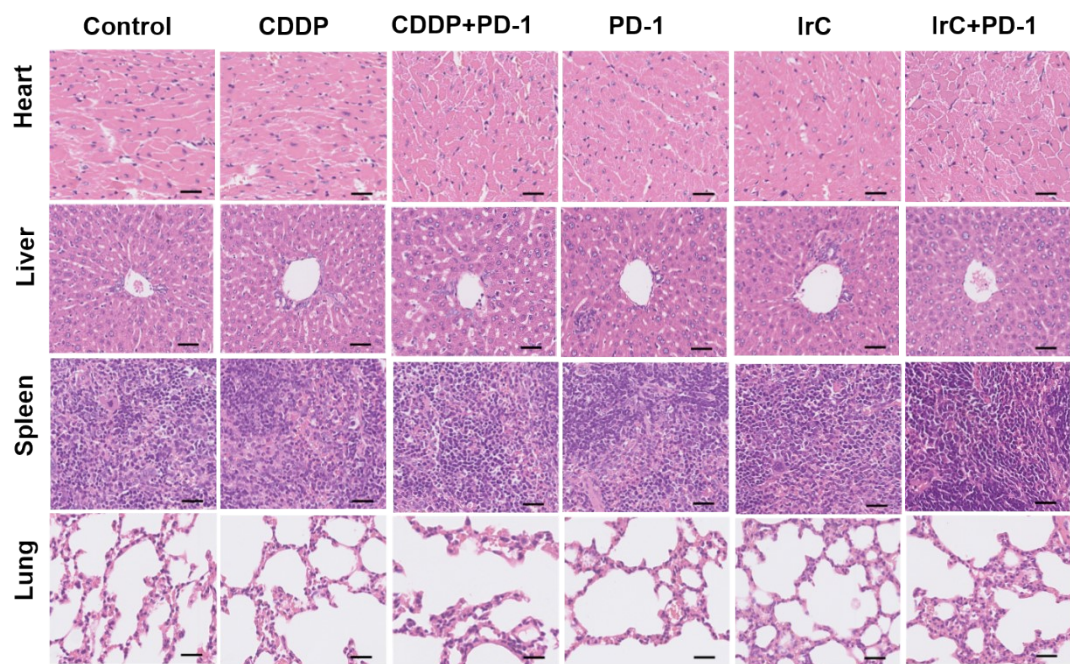


**Fig. S11** H&E staining of the main organ slices collected from the mice under different treatment. Scale bars: 100  $\mu$ m.

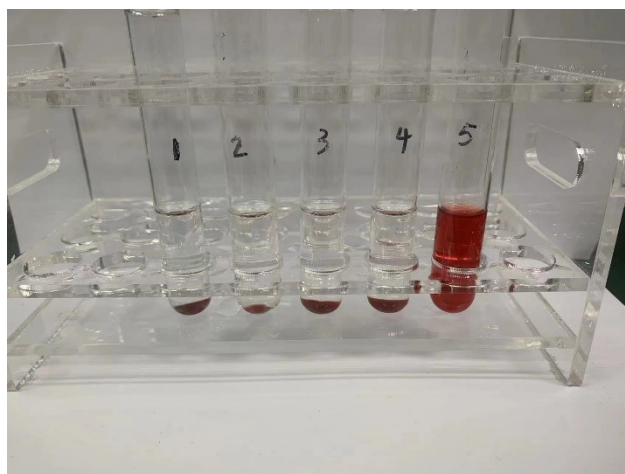


**Fig. S12** Hemolysis assay of IrC with different concentrations. 1: Normal saline, 2: IrC 5  $\mu$ M, 3: IrC 10  $\mu$ M, 4: IrC 20  $\mu$ M, 5: distilled water.